Volume 24, No 3 | International Journal of Radiation Research, July 2026

Effects of ginsenoside Rg3 on chemoradiosensitivity to paclitaxel in breast cancer cells and its correlation with autophagy-related genes

S. Chen[1], Y. Liu[1], H. Bao[1], E. Zhao[1], X. Qiao[2], M. Gu[1], J. Zhou[1], J. Zhang[3*]

[1]Department of Thoracic Surgery and Department of Tumor Surgery II, The Second Affiliated Hospital of Qiqihar Medical University, Qiqihar, Heilongjiang Province, China
[2]School of Pharmacy, Qiqihar Medical College, Qiqihar, Heilongjiang Province, China
[3]Departments of Neurology, The Second Affiliated Hospital of Qiqihar Medical University, Qiqihar, Heilongjiang Province, China

► *Original article*

***Corresponding author:**
Jingyan Zhang, Ph.D.
E-mail:
zhangjingyan1982@126.com

Received: November 2025
Final revised: February 2026
Accepted: February 2026

Int. J. Radiat. Res., July 2026; 24(3): 713-721

DOI: 10.61186/ijrr.24.3.18

Keywords: *Ginsenoside Rg3, paclitaxel, breast cancer; autophagy, drug resistance Wnt/β-catenin, radiosensitization, radiotherapy-related resistance.*

ABSTRACT

Background: Resistance to paclitaxel (PTX) remains is a challenge in treatment of breast cancer, which is often mediated by multidrug resistance proteins and dysregulated autophagy. Ginsenoside Rg3 has been reported to enhance chemosensitivity in several malignancies, but its role in PTX resistance and underlying mechanisms in breast cancer remain unclear. ***Materials and Methods:*** In this study Human breast cancer MCF-7 cells treated with PTX, Rg3, or both. Cell viability was assessed by MTT assay, apoptosis by Annexin V/PI flow cytometry, and drug efflux by rhodamine-123 retention. Autophagy was evaluated using transmission electron microscopy, monodansylcadaverine and acridine orange staining, and Western blot analysis of autophagy-related proteins. Expression of MDR1/P-glycoprotein and Wnt/β-catenin signaling components was also analyzed. ***Results:*** Rg3 significantly enhanced PTX-induced growth inhibition and apoptosis in MCF-7 cells compared with PTX alone. Combination treatment increased intracellular rhodamine-123 accumulation, indicating reduced drug efflux. Autophagy activation was evidenced by increased LC3-II/LC3-I ratio and Beclin-1 expression, along with decreased p62 levels. Additionally, Rg3 combined with PTX downregulated MDR1/P-glycoprotein and suppressed key proteins of the Wnt/β-catenin signaling pathway. Correlation analysis revealed that autophagy markers were positively associated with apoptosis and negatively correlated with MDR1 expression. ***Conclusion:*** Ginsenoside Rg3 increases breast cancer cells chemosensitivity to paclitaxel, potentially through modulation of autophagy, inhibiting Wnt/β-catenin signaling, and suppressing multidrug resistance mechanisms. The findings of this study showed that Rg3 may represent a potential adjuvant for chemotherapy, while its role in modulating radiosensitivity needs further investigation in dedicated radiotherapy models.

INTRODUCTION

Breast cancer (BC) continues to be the most common malignant tumor among women globally, with a visible burden of morbidity and mortality. Data from the Global Cancer Observatory (GLOBOCAN) indicate that in 2022, BC accounted for approximately 23.8% to 29% of new female cancer cases, with an estimated 2.3 million new cases and 660,000 to 670,000 deaths, posing a severe threat to women's health [1].

Despite advances in early diagnosis and comprehensive treatment options for BC chemotherapy remains an essential treatment for advanced BC, particularly with taxanes such as paclitaxel (PTX) [2]. In clinical practice, PTX-based chemotherapy is frequently combined with radiotherapy as part of multimodal treatment strategies. PTX, a commonly used microtubule stabilizer, continues to be a standard regimen in metastatic BC, extending progression-free survival (PFS) and improving objective response rate (ORR) [3]. However, tumor cells often develop multidrug resistance (MDR) during treatment, limiting the efficacy of PTX and even leading to treatment failure [4, 5]. Importantly, many of the molecular mechanisms that underlie chemoresistance - such as enhanced DNA damage repair, prosurvival signaling, and adaptive autophagy - are also implicated in radioresistance, thereby affecting the overall efficacy of combined chemoradiotherapy.

The mechanisms of MDR are complex, involving overexpression of drug efflux pumps, defects in apoptosis pathways, and regulation by the tumor microenvironment [6]. Among these, the MDR1 gene-encoded P-glycoprotein (P-gp) can be highly expressed under activation of the Wnt/β-catenin (β-cat) pathway, where Wnt ligands binding to Frizzled

[Downloaded from ijrr.com on 2026-11-15]

[DOI: 10.66224/ijrr.24.3.18]

receptors promote β-cat nuclear translocation and MDR1 transcription [7]. This mechanism is particularly prominent in PTX-resistant cells, characterized by co-upregulation of Frizzled receptor 1 (FZD1) and P-gp [8]. Autophagy can clear damaged structures and promote survival but may also enhance chemotherapy toxicity through inhibition [9, 10]. At the same time, radiation-induced stress is known to trigger autophagy as an adaptive response, which can either protect tumor cells or contribute to cell death, depending on the context. Notably, there is a close interaction between autophagy and the Wnt/β-cat pathway [11], and both pathways have been implicated in the development of chemo- and radioresistance, making them important targets for combined intervention.

Ginsenoside Rg3 (G-Rg3), a major active component of ginseng and a diol-type triterpenoid saponin, has garnered attention for its anticancer potential. Studies have shown that Rg3 not only directly inhibits tumor cell proliferation and induces apoptosis but also enhances chemosensitivity by regulating the autophagy pathway and reversing MDR [12]. Rg3 visibly downregulates the expression of key molecules in the Wnt/β-cat pathway, β-cat and FZD1, thereby inhibiting MDR1/P-gp-mediated drug efflux [13]. A 2024 study reported that combining Rg3 with near-infrared photothermal therapy in doxorubicin-resistant BC cells visibly reduced the activity of the PI3K/Akt/mTOR pathway, increased drug accumulation and apoptosis rate (AR), and reversed the drug-tolerant phenotype [14]. Additionally, in models of liver and lung cancer, Rg3 upregulated the expression of key autophagy genes such as LC3-II, Beclin-1, and Atg5, thereby regulating mitophagy and exacerbating tumor cell death [15]. These multifaceted effects suggest that G-Rg3 may act not only as a chemosensitizer but also as a potential modulator of pathways that participate in radioresistance. Although studies have explored the combined effects of G-Rg3 and PTX on BC, the role of the Wnt/β-cat–MDR1/P-gp axis in PTX resistance and the molecular mechanisms by which Rg3 reverses resistance through this pathway remain understudied. Particularly, how Rg3 coordinates the interaction between autophagy and the Wnt/β-cat pathway in the context of treatment resistance requires further elucidation.

Based on the above research background, this article aims to systematically investigate the chemosensitization effects of G-Rg3 in PTX-induced BC cells and further elucidate its regulatory mechanisms on the Wnt/β-cat pathway. Additionally, by analyzing the expression of autophagy-related genes, this article explores whether Rg3 coordinates the interaction between the Wnt/β-cat signaling and autophagy pathways to inhibit PTX resistance and increase drug accumulation and apoptosis levels. Because these pathways are critically involved in both chemo- and radioresistance, the present study provides a new molecular basis and theoretical foundation not only for anti-resistance treatment strategies combining Rg3 and PTX, but also for future exploration of G-Rg3 as a potential adjunct in chemoradiotherapy for breast cancer.

MATERIALS AND METHODS

The experimental design focused on evaluating the effects of G-Rg3 on paclitaxel chemosensitivity and the regulation of autophagy, MDR1/P-gp, and Wnt/β-catenin signaling in MCF-7 breast cancer cells. Because these pathways also play essential roles in determining tumor responses to radiotherapy, the methods used here provide mechanistic insight that may be relevant for understanding both chemo- and radioresistance, even though no radiation exposure was applied in this study.

Cell culture

RPMI-1640 medium (Hyclone, USA) supplemented with 10% fetal bovine serum (FBS) (Gibco, USA) and 1% penicillin-streptomycin solution (Gibco, USA) was used to cultivate the human BC cell line MCF-7, which was acquired from the Cell Bank of the Chinese Academy of Sciences, China. The cells were regularly cultivated at 37°C, 5% CO2, and 95% relative humidity in an incubator (Thermo Fisher Scientific, USA) with a 1:3 passage ratio. Fresh media was supplied every two to three days.

Pre-experiment for PTX IC_{50} concentration

Based on the reported inhibitory effects of PTX on MCF-7 cells [16], a concentration gradient of 0.01, 0.1, 1, 10, and 100 nM was set. MCF-7 in a 96-well plate (5×10^3 per well) were cultured (24 h) to ensure cell adhesion. The medium was then replaced with one containing different concentrations of PTX, with six replicates per group. After further cultivation (48 h), cell viability (CV) was assessed, and the inhibition rate was calculated. The dose-response curve was fitted using GraphPad Prism software to determine the IC_{50} value of PTX in MCF-7.

Drug preparation and treatment

PTX was purchased from Sigma-Aldrich (USA, catalog number: T7191) and dissolved in analytical grade dimethyl sulfoxide (DMSO) (≥99.9%, Sinopharm, catalog number: D837300) to generate a 10 mM stock solution, and aliquots were stored (-20℃, in the dark). Before use, it was subjected to dilution with the culture medium to the IC_{50} concentration. G-Rg3 (purity ≥98%, Wuhan Tianzhi Biotechnology Co., Ltd. China, batch number: TZ202301) was subjected to dissolution in analytical grade DMSO to generate a 100 μM stock solution (based on preliminary experiments), which was stored (-20℃, in the dark). All stock solutions were

[Downloaded from ijrr.com on 2026-11-15]

[DOI: 10.66224/ijrr.24.3.18]

thoroughly vortexed before use and diluted in complete culture medium as needed, ensuring the final DMSO concentration did not exceed 0.1% to avoid nonspecific toxicity to cells.

Cell treatment and grouping

Logarithmically growing MCF-7 cells were subjected to drug intervention experiments as follows, with all experiments set up with at least three biological replicates and a uniform culture time of 48 h.

Control group (AG): Routine culture medium without DMSO or drug treatment.

PTX (IC_{50}=5.2 nM) group (BG): Treated with PTX at the IC_{50} concentration (determined in Section 2.2) for 48 h.

G-Rg3 (100 μM) group (CG): Treated with G-Rg3 at 100 μM for 48 h.

G-Rg3+PTX group (DG): Pre-treated with G-Rg3 (100 μM) for 24 h, followed by co-incubation with PTX (IC_{50} concentration) for another 24 h.

PTX+Rapamycin group (EG): Treated simultaneously with PTX (IC_{50}) and rapamycin (100 nM, a classic autophagy inducer targeting mTOR, Sigma-Aldrich, catalog number: R0395) to verify the autophagy-mediated enhancement of drug efficacy.

MTT assay for determination of drug resistance index

MCF-7 cultured for 48 h were collected and 20 μL of 5 mg/mL MTT solution (Sigma-Aldrich, USA) was applied. After incubation (37°C, 4 h), the supernatant was removed and 150 μL of DMSO was applied. The cells were shaken thoroughly (10 min) for dissolving the purple formazan crystals. OD_{570} was subjected to measurement adopting a microplate reader (BioTek, USA), with background correction at 630 nm. The cell inhibition rate was calculated after subtracting the background from the blank wells (no cells).

Rhodamine-123 retention assay for assessment of drug resistance

Treated MCF-7 were seeded in plates (6 wells). When the confluence was 70%-80%, the culture medium was removed and replaced with medium containing 10 μg/mL Rh123 dye (Sigma-Aldrich, USA). At 37°C for 1.5 h (avoiding light), after staining, three rinses were carried out with sterile PBS (Thermo Fisher Scientific, USA) to remove free dye, followed by incubation in colorless RPMI-1640 medium (Cytiva, USA) (30 min). Fluorescence distribution was observed and images were captured adopting the relative device (Leica DMi8, Leica Microsystems, Germany). The average fluorescence intensity (FI) in five randomly selected fields was measured adopting ImageJ software (NIH, USA). Higher FI indicated more Rh123 retention, suggesting weaker efflux function and lower drug resistance, while weaker fluorescence indicated enhanced dye efflux and stronger MDR. The experiment was repeated three times, and the average value was used for statistical analysis to compare changes in drug resistance.

Apoptosis analysis

Floating and adherent cells were collected after the treatment. The cells were washed twice using pre-cooled PBS and resuspended in binding buffer. Based on the guidance of the kit (BD Biosciences, San Jose, CA, USA), 5 μL of Annexin V-FITC and 5 μL of PI were applied to each tube (avoiding light, 25°C, 15 min). 400 μL of binding buffer was applied to ensure homogeneity. Analysis was carried out within 1 h adopting a flow cytometer (BD FACSCanto II, BD Biosciences, USA) with excitation wavelengths of 488 nm (FITC) and 535 nm (PI) and emission wavelengths of 530 nm (FITC) and 617 nm (PI). No fewer than 10,000 cell events were collected. Data were analyzed adopting FlowJo software (Tree Star Inc., Ashland, OR, USA) to distinguish apoptosis stages based on Annexin V and PI staining: early apoptotic cells were Annexin V^+/PI^-, and late apoptotic or necrotic cells were Annexin V^+/PI^+. Three independent experiment sets (at least) were conducted, and the AR was statistically compared among different drug treatments.

Detection of autophagy activity

(1) Observation of autophagosomes: MCF-7 intervened for 48 h were prepared into a single-cell suspension at 1×10^6/mL. Following glutaraldehyde fixation (2.5%, 4°C, 2 h; Servicebio, China) and PBS rinses (3 × 10 min), samples were post-fixed with 1% OsO_4 (Ted Pella, USA) for 2 h. After distilled water rinses (3 × 10 min), the cells were dehydrated with a gradient of 30%–100% ethanol, and acetone substitution were performed. The cells were embedded in pure Epon resin (SPI Supplies, USA), trimmed, and sectioned into 70-90 nm ultrathin slices, stained with uranyl acetate and lead citrate, and observed under a transmission electron microscope (Hitachi HT7800, Japan) to record images of autophagic structures.

(2) MDC fluorescence staining: MCF-7 after 48 h of intervention were incubated with fresh medium containing 50 μmol/L MDC working solution (Sigma-Aldrich, USA) (37°C, 5% CO_2, avoiding light, 10 min). Following PBS rinses (twice) (Gibco, USA), 4% paraformaldehyde (Servicebio, China) was adopted for fixation (15 min), and rinse was carried out again. Fluorescence spots related to autophagy were acquired through the relative device (Leica DMi8, Germany) with UV excitation light.

(3) Acridine orange (AO) staining: Treated MCF-7 were rinsed, and 1 μg/mL AO solution (Sigma-Aldrich, USA, dissolved in complete medium) was applied for incubation (37°C, 15 min). Following

[Downloaded from ijrr.com on 2026-11-15]

[DOI: 10.66224/ijrr.24.3.18]

rinsing three times, a fluorescence microscope (excitation wavelength 450-490 nm, emission wavelength above 520 nm) was adopted for observation. Red fluorescence indicated the accumulation of acidic vesicles, while green fluorescence indicated cytoplasmic and nuclear staining. The changes in the red/green fluorescence ratio in the images were analyzed adopting Photoshop software (Adobe, USA) to assess autophagy activity.

Western blot (WB) detection

Total protein was extracted from treated MCF-7 adopting RIPA buffer (Beyotime Biotechnology, China) with inhibitors and quantified via BCA method (Thermo Scientific, USA). 30 μg of protein from each sample were separated by 10%-12% SDS-PAGE, and PVDF membrane (Millipore, USA) transfer was carried out. 5% skim milk (dissolved in TBST) was adopted for blocking (1 h), and first antibodies (Ab) were applied (overnight, 4°C). The first Ab included Beclin-1, LC3-I, LC3-II, p62 (SQSTM1), MDR1, P-gp, FZD1, β-cat, GSK-3β, p-GSK-3β, and GAPDH (as an internal reference), all purchased from Cell Signaling Technology (USA) or Abcam (UK) and prepared at the dilution ratios recommended in the instructions. The next day, HRP-conjugated goat anti-rabbit secondary Ab (ZSGB-Bio, China) were applied (25°C, 1 h), followed by development with an ECL kit (Bio-Rad, USA) and band image acquisition adopting a gel imaging system. The protein expression levels were analyzed by ImageJ software (NIH, USA) for grayscale values, and target/GAPDH band intensity ratio was determined. All experiments were repeated independently three times.

Statistical methods

Data in this article were analyzed adopting SPSS 26.0, represented as mean ±SD. One-way ANOVA was adopted for intergroup contrast, and Tukey's post-hoc test was applied for pairwise contrast. CV and IC_{50} values after drug treatment were computed and plotted adopting GraphPad Prism 9.0 software. To explore the relationship between autophagy and apoptosis, Pearson correlation analysis (PCA) was adopted, with the correlation coefficient r indicating the degree of correlation. The difference was statistically considerable with $P<0.05$.

RESULTS

Determination of PTX IC_{50} concentration

The IC_{50} value of PTX for MCF-7 cells was determined by the MTT assay. The results suggested that the IC_{50} value of PTX after 48 h of treatment was 5.2 ± 0.3 nM (figure 1). Based on this result, 5 nM PTX was adopted as the standard.

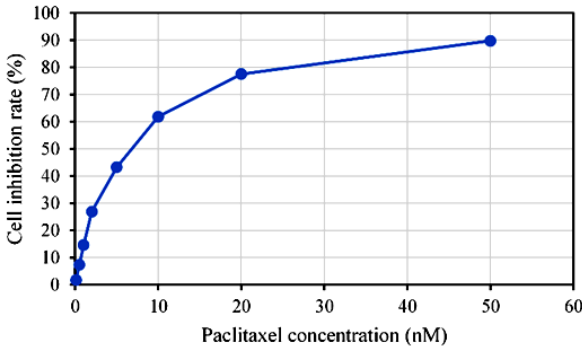


Figure 1. Effect of drugs on CV (MTT results).

G-Rg3 enhancing the cytotoxicity of PTX

The inhibition rate in the BG was found to be 42.5 ± 3.6% by MTT assay. The inhibition rate in the CG was visibly lower at 18.7 ± 2.1%, while that in the DG was visibly increased to 68.3 ± 4.2% (P < 0.05). Additionally, the inhibition rate in the EG was 65.8 ± 3.9%, which was similar to that in the DG, suggesting that autophagy regulation might be involved in the sensitization effect (table 1).

Table 1. Contrast of cell inhibition rates.

Grouping	Inhibition rate (%)	In contrast to BG(P)
AG	-	-
BG	42.5 ± 3.6	-
CG	18.7 ± 2.1	0.002
DG	68.3 ± 4.2	0.000
EG	65.8 ± 3.9	0.000

Effect of G-Rg3 on drug resistance

The results of the Rhodamine-123 retention assay suggested that as against the AG, the average FI of MCF-7 cells in the BG was visibly decreased (902 ± 120 vs. 1206 ± 150). The FI in the CG was visibly increased (1450 ± 180) (P<0.05). As against the BG, the FI in the DG was visibly increased (902 ± 120 vs 1653 ± 200, P<0.01), while the EG also exhibited higher FI (1556 ± 170), with no visible distinction from the DG (figure 2).

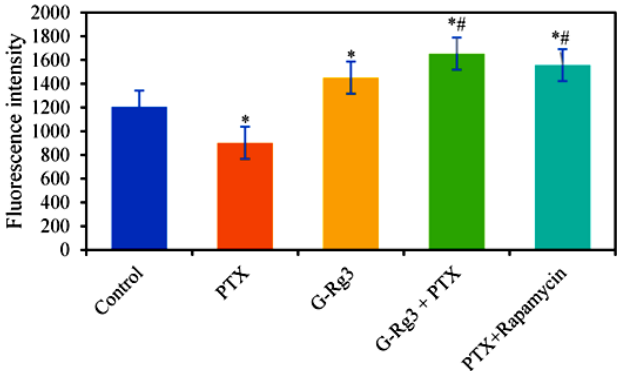


Figure 2. Comparison of FI of cells. (Note: "*" as against AG, "#" as against BG, P <0.05).

Analysis of AR of MCF-7 under different treatment conditions

The AR of cells in the AG was (5.4% ± 0.8%). As against the AG, the AR in the BG increased to (24.6% ± 2.1%), and the AR in the CG rose to (11.3% ± 1.4%) (P<0.05). As against the BG, the AR in the DG was

[Downloaded from ijrr.com on 2026-11-15]

[DOI: 10.66224/ijrr.24.3.18]

visibly higher (42.7% ± 3.6%, P<0.01), and the AR in the EG also increased visibly (39.1% ± 2.8%), which was comparable to that in the DG (figure 3).

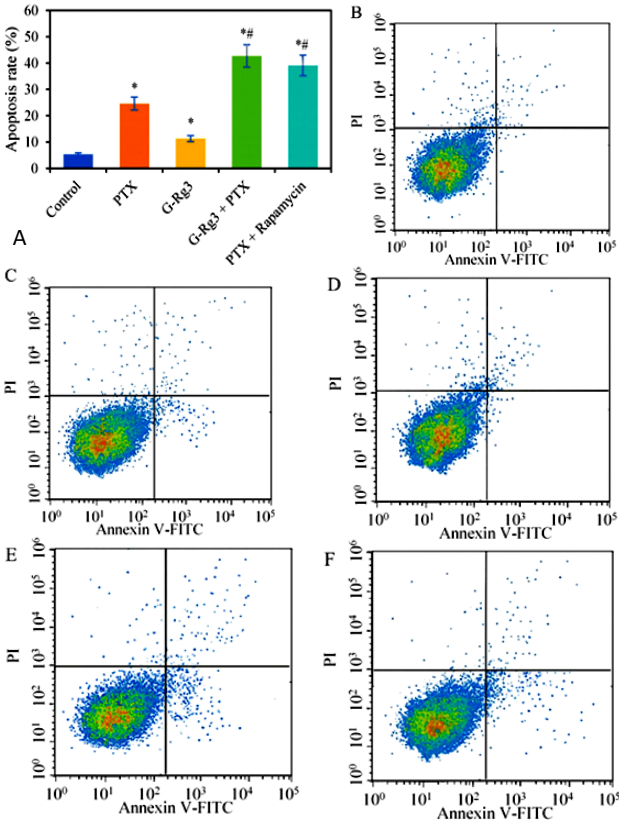


Figure 3. AR of MCF-7 under different drug treatment conditions. (Note: A: Contrast of AR; B-F: FlowJo analysis of Annexin V-FITC/PI apoptosis in MCF-7 in AG, BG, CG, DG, and EG. "*" as against AG, "#" as against BG, P <0.05).

Analysis of autophagy activity in MCF-7 under different treatment conditions

Transmission electron microscopy revealed that MCF-7 cells in the AG had intact morphology with few autophagosomes in the cytoplasm; the BG exhibited a small number of autophagic structures with membranous changes; G-Rg3 monotherapy slightly increased the number of autophagosomes, but no visible changes were observed; in contrast, the DG had a visible increase in autophagosomes, with multiple typical double-membrane structures visible in the cytoplasm, which was visibly higher than that in the monotherapy groups; the EG had the strongest autophagy activity (figure 4-A). MDC and AO staining results suggested that as against the AG, the number of MDC-positive spots and the red/green fluorescence ratio in the BG and CG were visibly increased; as against the BG, the number of positive spots and the red/green fluorescence ratio in the DG and EG were visibly increased (P < 0.05). No visible distinction was noted between the DG and EG (P>0.05) (figure 4-B~C).

Changes in autophagy and drug resistance protein expression under different treatment conditions

WB analysis revealed that in terms of autophagy-related proteins, as against the AG, there were slight changes in Beclin-1, the LC3-II/I ratio, and p62 in the BG and CG, but no visible distinctions were noted (P>0.05). In contrast, as against the BG, the DG and EG suggested visible increases in Beclin-1 and the LC3-II/I ratio, and a visible decrease in p62. Regarding MDR-related proteins, as against the AG, MDR1/P-gp was visibly elevated in the BG. As against the BG, MDR1/P-gp was markedly reduced in the DG and EG (P < 0.05). In terms of Wnt/β-cat pathway protein expression, as against the AG, there were slight changes in FZD1, β-cat, and p-GSK-3β in the BG and CG (P>0.05). As against the BG, FZD1, β-cat, and p-GSK-3β were markedly decreased in the DG and EG (P<0.05). The DG and EG had similar levels of the aforementioned indicators, with no visible statistical distinctions; GSK-3β expression suggested no visible statistical distinctions among the groups (P>0.05) (figure 5).

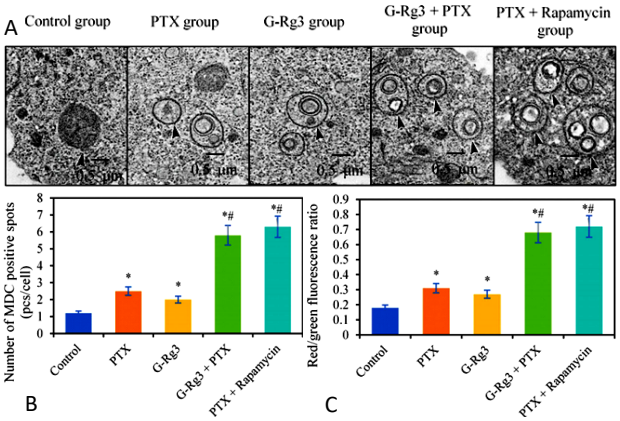


Figure 4. Contrast of autophagy activity in MCF-7 under different treatment conditions. (**A:** Transmission electron microscopy images; **B:** MDC staining results; **C:** AO staining results; "*" as against AG, "#" as against BG, P<0.05).

Correlation analysis between autophagy marker expression levels and AR

The results of PCA (table 2) suggested that the LC3-II/I ratio, an autophagy marker, had a markedly positive correlation with the AR (r = 0.82, P=0.003). The expression level of Beclin-1 had a markedly positive correlation with the AR (0.76, 0.008). p62, a substrate for autophagic degradation, had a visible negative correlation between its expression level and the AR (-0.69, 0.012). Regarding drug resistance-related proteins, the expression level of MDR1/P-gp was markedly negatively correlated with the AR (-0.71, 0.010). Among the key molecules of the Wnt/β-cat pathway, FZD1 (-0.65, 0.018), β-cat (-0.68, 0.014), and p-GSK-3β (-0.63, 0.021) all had visible negative correlations with the AR.

[Downloaded from ijrr.com on 2026-11-15]

[DOI: 10.66224/ijrr.24.3.18]

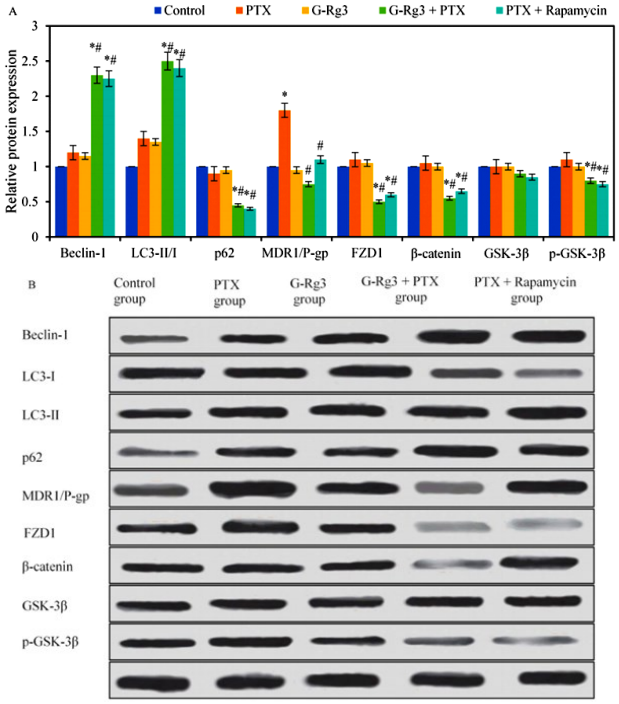


Figure 5. Changes in autophagy and drug resistance protein expression in MCF-7 under different treatment conditions (**A:** Contrast of relative protein expression results; **B:** WB band image; "*" as against AG, "#" as against BG, P<0.05).

Table 2. PCA between autophagy markers, drug resistance proteins, Wnt/β-cat pathway molecules, and AR.

Test indicators	Correlation coefficient (*r*)	*P*	Direction of correlation
LC3-II/Iratio	0.82	0.003	Positive correlation
Beclin-1	0.76	0.008	Positive correlation
p62	-0.69	0.012	Negative correlation
MDR1/P-gp	-0.71	0.010	Negative correlation
FZD1	-0.65	0.018	Negative correlation
β-cat	-0.68	0.014	Negative correlation
p-GSK-3β	-0.63	0.021	Negative correlation

DISCUSSION

This article systematically explored the effects of G-Rg3 on the chemosensitivity of PTX-induced BC cells and its association with autophagy. The results demonstrated that G-Rg3 markedly enhanced the cytotoxicity of PTX against MCF-7 cells, increased the apoptosis rate (AR), and reversed drug resistance by modulating autophagy activity and the Wnt/β-catenin pathway. Because these pathways are also critically involved in radioresistance, the present findings provide additional mechanistic insights that may be relevant for improving responses not only to chemotherapy but also to radiotherapy in BC.

Firstly, the MTT assay results indicated that the combination of G-Rg3 and PTX markedly increased the cell proliferation inhibition rate to 68.3%. The AR also increased to 42.7%. G-Rg3 may enhance the chemotherapeutic effect of PTX through a mechanism similar to rapamycin-induced autophagy activation. This is consistent with studies showing that Rg3 enhances the effects of chemotherapeutic drugs through autophagy regulation [12]. Liposomal formulations of Rg3 have been shown to enhance the anti-metastatic efficacy of docetaxel by increasing capture of circulating tumor cells and disrupting metastatic niches [16], aligning closely with the observations in this study. Because radiotherapy often relies on apoptosis induction and is influenced by the same survival pathways that modulate chemosensitivity, enhanced apoptotic signaling may also have implications for improving radiosensitivity.

In terms of mechanism, the Rhodamine-123 retention assay revealed that G-Rg3 markedly inhibited P-gp-mediated drug efflux, resulting in an 83.3% increase in intracellular PTX accumulation in the combined treatment group compared with the BG. This finding is consistent with a triple-negative BC study [17], which confirmed that G-Rg3 downregulates P-gp expression and blocks its function. MDR1/P-gp is not only a central determinant of chemotherapy resistance but also contributes to radioresistance by reducing treatment-induced intracellular stress. The marked reduction in MDR1/P-gp observed in the DG and EG groups suggests that G-Rg3 may counteract resistance mechanisms relevant to both treatment modalities. Supporting this, G-Rg3 has also been reported to promote MDR1 ubiquitination and degradation [18].

Autophagy is widely recognized as a context-dependent stress response that may be cytoprotective (facilitating metabolic adaptation and drug tolerance) or, under conditions of sustained or excessive activation, contribute to autophagy-dependent cell death (ADCD) sometimes referred to as "autophagic cell death" [19]. In the present study, ginsenoside Rg3 enhanced paclitaxel-mediated growth inhibition and apoptosis concomitantly with increased autophagy-associated signals (LC3-II/LC3-I and Beclin-1 upregulation with p62 reduction and increased acidic/autophagic vacuole staining). While these findings are consistent with a pro-death autophagic response, it is also plausible that autophagy initially represents an adaptive survival mechanism that—once surpassing a stress "threshold"—becomes maladaptive and contributes to loss of cellular viability and death programs [20]. Importantly, current consensus guidelines emphasize that increases in autophagy markers alone do not establish causality for ADCD; demonstrating an autophagy-dependent death mechanism typically requires showing that genetic or pharmacologic inhibition of autophagy rescues viability (or reduces death) under the same conditions [21]. In addition, a distinct subtype of autophagy-dependent death termed autosis has been described, characterized by autophagy gene dependence and regulation by Na^+/K^+-ATPase [22].

Additionally, this study confirmed that G-Rg3 can enhance PTX-induced apoptosis by activating

[Downloaded from ijrr.com on 2026-11-15]
[DOI: 10.66224/ijrr.24.3.18]

autophagy. Transmission electron microscopy, MDC, and AO staining showed visible increases in autophagosome formation and acidic vesicle accumulation, and WB results indicated enhanced autophagic flux. The positive correlation between autophagy markers (Beclin-1, LC3-II/I) and AR, together with the negative correlation with p62, further supports the hypothesis that "G-Rg3 promotes PTX-induced apoptosis by activating autophagy." Autophagy is known to play a dual role in cancer therapy. After radiotherapy, autophagy is often activated as a cytoprotective mechanism that enhances tumor cell survival, although excessive autophagy can promote cell death. Various ginsenosides, including Rg3 and Rh4, modulate ROS-dependent autophagy pathways [23]. G-Rg3 specifically activates autophagy and inhibits cell survival in MCF-7 cells through the p62/mTOR pathway [24]. These findings suggest that the autophagy-regulating activity of G-Rg3 might also influence radiosensitivity and deserves further investigation.

A key translational consideration is that the present study evaluated a single Rg3 concentration (100 μM). Although this dose is consistent with concentrations commonly used in mechanistic in-vitro studies of Rg3, dose–response characterization is required to determine whether chemosensitization is concentration-dependent and to define a potential therapeutic window. Future experiments should test multiple Rg3 concentrations (e.g., 25, 50, and 100 μM) in combination with paclitaxel, quantify drug interaction using established synergy frameworks (e.g., combination index/isobologram approaches), and include non-malignant breast epithelial cells to assess selectivity. Such analyses would clarify the minimum effective concentration for sensitization and whether higher doses introduce off-target cytotoxicity [25].

Finally, this article found that G-Rg3 enhances the anti-tumor activity of PTX by inhibiting the Wnt/β-catenin pathway. The combination of G-Rg3 and PTX or co-use with rapamycin markedly downregulated the expression of FZD1, β-catenin, and p-GSK-3β, and the levels of these molecules were negatively correlated with AR. The Wnt/β-catenin pathway promotes tumor progression in BC and osteosarcoma and is closely associated with drug tolerance [26]. Importantly, Wnt/β-catenin signaling is also a recognized mediator of radioresistance due to its roles in stemness maintenance, DNA repair, and survival signaling. Other studies have confirmed that G-Rg3 inhibits tumor proliferation and metastasis by suppressing the Wnt/β-catenin signal [27, 28]. Thus, inhibition of Wnt/β-catenin by G-Rg3 in this study further supports its potential relevance as a modulator of both chemo- and radioresistance.

β-Catenin has been shown to bind *T-cell* factor/ lymphoid enhancer factor (TCF/LEF) elements within the MDR1 promoter, thereby enhancing P-glycoprotein expression and drug efflux capacity. In the present study, ginsenoside Rg3 treatment was associated with concomitant suppression of Wnt/β-catenin pathway components and downregulation of MDR1/P-glycoprotein expression, together with increased intracellular rhodamine-123 accumulation. Based on these findings, we propose a testable mechanistic hypothesis in which Rg3 inhibits Wnt/β-catenin signaling, leading to reduced MDR1 transcription, diminished P-glycoprotein–mediated paclitaxel efflux, increased intracellular drug accumulation, and enhanced apoptotic response. Although this signaling hierarchy cannot be conclusively established from the current data, it provides a biologically plausible framework that integrates our molecular and functional observations and can be directly evaluated in future studies using Wnt pathway modulation or MDR1-specific interventions.

While the present study was not designed to establish causal hierarchy among signaling pathways, our findings allow the proposal of a testable mechanistic model for the chemosensitizing effect of ginsenoside Rg3. Based on the observed downregulation of Wnt/β-catenin signaling components, reduced MDR1/P-glycoprotein expression, enhanced autophagic activity, and increased apoptosis, we speculate that Rg3 may primarily suppress Wnt/β-catenin signaling, which in turn leads to attenuation of MDR1/P-glycoprotein–mediated drug efflux and concomitant modulation of autophagy. Inhibition of Wnt/β-catenin signaling has been reported to negatively regulate P-glycoprotein expression and to interact with autophagy-related pathways, thereby influencing cell survival and apoptotic responses. Alternatively, Rg3-induced autophagy may represent an upstream event that enhances paclitaxel-induced apoptosis and secondarily affects Wnt/β-catenin signaling and multidrug resistance mechanisms. While both models are consistent with our correlative data, further studies using pathway-specific inhibitors, gene silencing approaches, and temporal analyses will be required to delineate the primary molecular target of Rg3 and the directionality of these signaling interactions.

Although this article provided experimental evidence for the combination of G-Rg3 and PTX in treating BC resistance, there are still limitations. First, only the MCF-7 BC cell line was used, lacking validation in other BC subtypes (e.g., HER2-positive or triple-negative BC) or in vivo models, which limits the generalizability of the findings [29]. Second, although the results suggest that G-Rg3 enhances PTX -induced apoptosis by activating autophagy, the precise interaction between autophagy-related pathways and apoptotic signaling remains unclear. Future studies using gene knockdown or

[Downloaded from ijrr.com on 2026-11-15]

[DOI: 10.66224/ijrr.24.3.18]

overexpression strategies could clarify these mechanisms. Third, because radiotherapy was not experimentally included, the potential radiosensitizing effects of G-Rg3 remain speculative. Dedicated studies incorporating ionizing radiation, clonogenic survival assays, and DNA damage markers would be needed to validate this possibility. Additionally, this article did not evaluate the pharmacokinetics, systemic toxicity, or tissue distribution of combined G-Rg3 and PTX treatment. Comprehensive preclinical evaluations are required to support translation toward clinical use.

CONCLUSION

This article demonstrated that G-Rg3 enhances the sensitivity of breast cancer MCF-7 cells to paclitaxel and reverses drug resistance by activating autophagy, inhibiting the Wnt/β-catenin signaling pathway, and downregulating MDR1/P-gp expression. These coordinated mechanisms collectively promote apoptosis, increase intracellular drug accumulation, and inhibit pro-survival signaling. Because autophagy regulation, Wnt/β-catenin inhibition, and MDR1 suppression are also key determinants of tumor radioresistance, the present findings provide a mechanistic basis suggesting that G-Rg3 may have broader potential as a sensitizing agent in combined chemo-radiotherapy. Although further studies incorporating ionizing radiation models are required, this work lays an important theoretical and experimental foundation for future development of G-Rg3–based strategies aimed at overcoming treatment resistance in breast cancer.

***Conflict of Interest Disclosure*:** All authors declare no financial or non-financial conflicts of interest.

***Ethical approval*:** This study used the human breast cancer cell line MCF-7 (purchased from the Cell Bank of the Chinese Academy of Sciences) and did not involve human or animal experiments, thus no ethical committee approval was required.

***Informed consent*:** This study did not involve human subjects or clinical data, and therefore an informed consent statement is not applicable.

***Data availability*:** All data generated or analyzed during this study are included in this manuscript. Additional data are available from the corresponding author upon reasonable request.

***Author contributions*:** Conceptualization: S.C.; Methodology: Y.L.; Data curation & Formal analysis: H.B.; Writing - original draft: E.Z.; Writing - review & editing: X.Q.; Funding acquisition: M.G.; Supervision: J.Z., J.Z.

***Funding*:** The research is supported by: This study was funded by the 2020 Heilongjiang Provincial Undergraduate Universities Basic Scientific Research Fund Scientific and Technological Research Project (Project No. 2020-KYYWF-0025).

REFERENCES

1. Zhang Y, Ji Y, Liu S, Li J, *et al.* (2025) Global burden of female breast cancer: New estimates in 2022, temporal trend and future projections up to 2050 based on the latest release from GLOBOCAN. *Journal of the National Cancer Center,* ***5****(3): 287-96*.
2. Jivani A and Shinde RK (2024) A comprehensive review of taxane treatment in breast cancer: clinical perspectives and toxicity profiles. *Cureus,* ***16****(4): e59266*.
3. Lu H, Zha S, Zhang W, Wang Q, *et al.* (2021) A systematic review and meta-analysis of nab-paclitaxel mono-chemotherapy for metastatic breast cancer. *BMC Cancer,* ***21****(1): 830*.
4. Duan C, Yu M, Xu J, Li BY, *et al.* (2023) Overcoming cancer multi-drug resistance (MDR): reasons, mechanisms, nanotherapeutic solutions, and challenges. *Biomedicine and Pharmacotherapy,* ***162****: 114643*.
5. Xu H, Li L, Dong B, Lu J, *et al.* (2023) TRAF6 promotes chemoresistance to paclitaxel of triple negative breast cancer via regulating PKM2-mediated glycolysis. *Cancer Medicine,* ***12****(19): 19807-20*.
6. Chen C, Bu X, Deng L, Xia J, *et al.* (2025) Astragaloside IV as a promising therapeutic agent for liver diseases: current landscape and future perspectives. *Frontiers in Pharmacology,* ***16****: 1574154*.
7. Alalawy AI (2024) Key genes and molecular mechanisms related to Paclitaxel Resistance. *Cancer Cell International,* ***24****(1): 244*.
8. Zhang H, Zhang X, Wu X, Li W, *et al.* (2012) Interference of Frizzled 1 (FZD1) reverses multidrug resistance in breast cancer cells through the Wnt/β-catenin pathway. *Cancer Letters,* ***323****(1): 106-13*.
9. Qin Y, Ashrafizadeh M, Mongiardini V, Grimaldi B, *et al.* (2023) Autophagy and cancer drug resistance in dialogue: Pre-clinical and clinical evidence. *Cancer Letters,* ***570****: 216307*.
10. Wang T, He M, Zhang X, Guo Z, *et al.* (2024) Deciphering the impact of circRNA-mediated autophagy on tumor therapeutic resistance: a novel perspective. *Cellular and Molecular Biology Letters,* ***29****(1): 60*.
11. Huang Y, Zhang R, Lyu H, Xiao S, *et al.* (2024) LncRNAs as nodes for the cross-talk between autophagy and Wnt signaling in pancreatic cancer drug resistance. *Int J Biological Sciences,* ***20****(7): 2698-726*.
12. Zhu Y, Wang A, Zhang S, Kim J, *et al.* (2023) Paclitaxel-loaded ginsenoside Rg3 liposomes for drug-resistant cancer therapy by dual targeting of the tumor microenvironment and cancer cells. *J Advanced Research,* ***49****: 159-73*.
13. Meng ZQ, Zhang R, Wu XW, Jin TF, Zhang MH (2022) Ginsenoside Rg3 regulates cisplatin resistance in gastric cancer by wnt/β-catenin signaling pathway. *Zhongguo yi xue ke xue yuan xue bao,* ***44****(3): 366-76*.
14. Chang Y, Fu Q, Lu Z, Jin Q, *et al.* (2024) Ginsenoside Rg3 combined with near-infrared photothermal reversal of multidrug resistance in breast cancer MCF-7/ADR cells. *Food Science and Nutrition,* ***12****(8): 5750-61*.
15. Liu Y, Li G, Ning J, Zhao Y (2024) Unveiling the experimental proof of the anticancer potential of ginsenoside Rg3 (Review). *Oncology Letters,* ***27****(4): 182*.
16. Xia J, Ma S, Zhu X, Chen C, *et al.* (2022) Versatile ginsenoside Rg3 liposomes inhibit tumor metastasis by capturing circulating tumor cells and destroying metastatic niches. *Science Advances,* ***8****(6): eabj1262*.
17. Nakhjavani M, Hardingham JE, Palethorpe HM, Tomita Y, *et al.* (2019) Ginsenoside Rg3: potential molecular targets and therapeutic indication in metastatic breast cancer. *Medicines,* ***6****(1): 17*.
18. Deng X, Wang J, Lu C, Zhou Y, *et al.* (2023) Updating the therapeutic role of ginsenosides in breast cancer: a bibliometrics study to an in-depth review. *Frontiers in Pharmacology,* ***14****: 1226629*.
19. Xu J, Elshazly AM, Gewirtz DA (2022) The Cytoprotective, Cytotoxic and Nonprotective Functional Forms of Autophagy Induced by Microtubule Poisons in Tumor Cells-Implications for Autophagy Modulation as a Therapeutic Strategy. *Biomedicines,* ***10****(7)*.
20. Jung S, Jeong H, Yu S-W (2020) Autophagy as a decisive process for cell death. *Experimental & Molecular Medicine,* ***52****(6): 921-30*.
21. Klionsky DJ, Abdel-Aziz AK, Abdelfatah S, Abdellatif M, *et al.* (2021) Guidelines for the use and interpretation of assays for monitoring autophagy (4th edition)(1). *Autophagy,* ***17****(1): 1-382*.

[Downloaded from ijrr.com on 2026-11-15]

[DOI: 10.66224/ijrr.24.3.18]

22. Liu Y, Shoji-Kawata S, Sumpter RM, Jr., *et al.* (2013) Autosis is a Na+,K+-ATPase-regulated form of cell death triggered by autophagy-inducing peptides, starvation, and hypoxia-ischemia. U S A. *Proc Natl Acad Sci,* ***110****(51): 20364-71*.
23. Li X, Cao D, Sun S, Wang Y (2023) Anticancer therapeutic effect of ginsenosides through mediating reactive oxygen species. *Frontiers in Pharmacology,* ***14****: 1215020*.
24. Jiang RY, Fang ZR, Zhang HP, Xu JY, *et al.* (2023) Ginsenosides: changing the basic hallmarks of cancer cells to achieve the purpose of treating breast cancer. *Chinese Medicine,* ***18****(1): 125*.
25. Peng Y, Zhang R, Yang X, Zhang Z, *et al.* (2019) Ginsenoside Rg3 suppresses the proliferation of prostate cancer cell line PC3 through ROS-induced cell cycle arrest. *Oncol Lett,* ***17****(1): 1139-45*.
26. Hashemi M, Hasani S, Hajimazdarany S, Ghadyani F, *et al.* (2023) Biological functions and molecular interactions of Wnt/β-catenin in breast cancer: Revisiting signaling networks. *Int J Biol Macromolecules,* ***232****: 123377*.
27. Mao X, Jin Y, Feng T, Wang H, *et al.* (2020) Ginsenoside Rg3 inhibits the growth of osteosarcoma and attenuates metastasis through the Wnt/β-Catenin and EMT signaling pathway. *Evidence-Based Complementary and Alternative Medicine,* ***2020****: 6065124*.
28. Wang X, Zeng W, Yang L, Chang T, Zeng J (2023) Epithelial-mesenchymal transition-related gene prognostic index and phenotyping clusters for hepatocellular carcinoma patients. *Cancer Genetics,* ***274-275****: 41-50*.
29. Li R, Liu H, Dilger JP, Lin J (2018) Effect of propofol on breast cancer cell, the immune system, and patient outcome. *BMC Anesthesiology,* ***18****(1): 77*.

[Downloaded from ijrr.com on 2026-11-15]

[DOI: 10.66224/ijrr.24.3.18]

[DOI: 10.66224/ijrr.24.3.18] [Downloaded from ijrr.com on 2026-11-15]